LASERS

PACS numbers: 42.55.Lt; 42.60.Lh; 52.80.–s
DOI: 10.1070/QE2011v041n04ABEH014402

Effect of SF_6 and NF_3 additives on UV and IR lasing in nitrogen

D.E. Genin, A.N. Panchenko, V.F. Tarasenko, A.E. Tel'minov

Abstract. **The lasing regimes of nitrogen laser on the $C^3\Pi_u - B^3\Pi_g$ transition with a high-energy long laser pulse under pumping by a transverse discharge in $N_2 - SF_6$ (NF_3) mixtures from generators with a semiconductor opening switch is studied. Laser pulses with two peaks and controlled delay between these peaks are obtained. It is shown that the time interval between the peaks may exceed 50 ns for $N_2 - NF_3$ mixtures. The conditions for obtaining effective UV lasing with a laser pulse width of more than 50 ns at the base level are determined. A possibility of depopulating the lower level of the $C^3\Pi_u - B^3\Pi_g$ transition by induced transitions in the first positive $B^3\Pi_g - A^3\Sigma_u^+$ system is shown; this process makes it possible to expand the pulse to 100 ns at λ = 337.1 nm. The highest lasing energy and power in the IR and UV spectral ranges are obtained for nitrogen lasers with spark preionisation.**

Keywords: *UV and IR nitrogen lasers, opening switch, effective lasing, NF_3 and SF_6 additives.*

1. Introduction

Nitrogen laser operates on self-terminating transitions and can generate nanosecond pulses at λ = 337.1 nm. Due to the low cost of working gas, simplicity of design, and reliability, nitrogen lasers are still used, despite their low output energy [1–4]. In addition, lasers on molecular nitrogen transitions are applied to study the new methods for implementing inversion and different pump regimes [5–10]. The results of numerous studies (see [5–17] and references therein) suggest that nitrogen lasers generate short pulses and must be pumped by generators based on capacitors and strip lines with low impedance, which form short excitation pulses. The highest lasing energy (40 mJ) on the $C^3\Pi_u - B^3\Pi_g$ band was obtained in [14] under pumping by a UV-preionised volume transverse discharge, and the highest lasing energy (5 mJ) on the $B^3\Pi_g - A^3\Sigma_g^+$ band at peak power of 0.4 MW was reported in [17].

To obtain inversion at a UV transition, the threshold electric field strength $E_0/p = U_0/(pd)$ in the laser gap (this field is determined by the applied voltage U_0, the interelectrode distance d, and the gas pressure p) should be no less than 100 V cm^{-1} Torr^{-1} [11]. When pumping a nitrogen laser by a transverse discharge using conventional generators with capacitance energy storages, inversion can be maintained for only a very short (no more than 5 ns) time, when the voltage across the laser gap decays. Addition of electronegative gases NF_3, F_2, and SF_6 to nitrogen slows down the gap voltage decay [11–17] and increases the E/p ratio in the steady-state discharge stage [6, 10, 18]. However, it is fairly difficult to form a volume discharge in nitrogen mixtures with electronegative gases using pumping by capacitance generators, and the total UV lasing time does not exceed ~30 ns [13–16]. Exceptions are studies [19, 20], where lasing pulses more than 100 ns wide at λ = 337.1 nm were reported. However, these results are difficult to analyse because no oscillograms of laser-gap voltage pulses and data on lasing energy were reported.

We showed that, using generators with opening switches (GOSs) to pump mixtures of nitrogen with electronegative gases, one can increase significantly the nitrogen laser pulse width and energy [6, 10]. When pumping by a transverse discharge, a two-peak regime was implemented for nitrogen laser, and UV lasing pulses with a width of about 50 ns were obtained [6]. In this paper we report the results of studying these regimes of nitrogen laser operation on the first and second positive nitrogen systems under GOS pumping. The purpose was to attain maximum lasing energies and search for new possibilities of controlling the laser pulse shape and width.

2. Experimental

The experiments were performed on lasers with GOS-excited transverse discharge and the active-medium length $\mathcal{L}$ = 72 or 90 cm, similar to those described in [6, 8, 10]. Their equivalent electric scheme is shown in Fig. 1. The pump generator con-

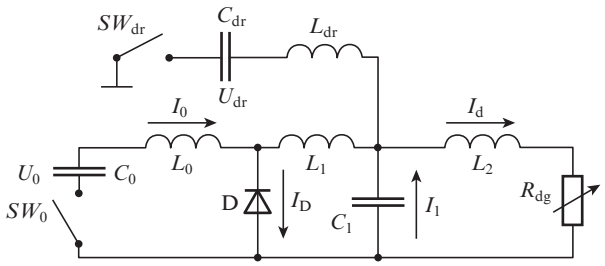

Figure 1. Equivalent electric scheme of a nitrogen laser pumped by an IES generator: (SW_0, SW_{dr}) controlled spark dischargers; (C_0) primary capacitance storage; (C_1) peaking capacitors; (C_{dr}) pump capacitance of SOS diodes in the forward direction (10 nF); (L_0, L_1, L_2, L_D) inductance contours; (R_{dg}) discharge gap resistance; (U_0, U_{dr}) charge voltages; (I_i) currents through contours; (D) SOS diodes.

D.E. Genin, A.N. Panchenko, V.F. Tarasenko, A.E. Tel'minov
Institute of High Current Electronics, Siberian Branch, Russian Academy of Sciences, prosp. Akademicheskii 2/3, 634055 Tomsk, Russia; e-mail: dm_genin@vtomske.ru, alexei@loi.hcei.tsc.ru, VFT@loi.hce.tsc.ru

Received 14 July 2010; revision received 10 February 2011
Kvantovaya Elektronika **41** (4) 360–365 (2011)
Translated by Yu.P. Sin'kov

tained main and auxiliary contours. The main contour was formed by a storage capacitor C_0 (70 or 160 nF), an inductance L_0, and a spark discharger SW_0. The auxiliary contour served to pump directly the semiconductor opening switch (SOS), which consisted of ten SOS diodes of the SOS-50-2 type, connected parallel to the peaking capacitors. The contour included a capacitor C_{dr} = 10 nF, a spark switch SW_{dr}, and an inductance L_{dr} = 3.13 μH. The discharge gap was preionised using the radiation from the spark gaps located symmetrically at both sides of the anode. Breakdown occurred in spark gaps under pulse charging of peaking capacitors C_1 (2.45 or 3.1 nF). The generator could operate either in the regime of energy storage in the contour inductance L_0 or as a conventional two-circuit LC generator. In the latter case the auxiliary contour was not used.

The characteristics of the gas discharge and laser radiation were investigated both for pure nitrogen and for N_2 mixtures with NF_3 and SF_6 in the pressure range of 10–100 Torr. The cavity mirrors were highly reflecting flat mirrors with an aluminum or dielectric coating and plane-parallel quartz or KRS-6 plates.

The nitrogen laser energy was measured by an OPHIR calorimeter with a PE-50BB sensor head. The pulse shape was measured by vacuum photodiodes FEK-22 SPU (UV spectral range) and FEK-29 SPU (IR range), onto which a part of radiation was directed using beamsplitters. Measurements were performed at a distance of 3–5 m from the laser output mirror. The radiation in the desired spectral range was cut by light filters. The spectrum of the laser radiation in the wavelength range of 200–850 nm was recorded by a StellarNet EPP2000-C25 spectrometer. Radiation pulses at the transitions in the first positive system of nitrogen were measured by the FEK-29 SPU photodiode, which was mounted on the output slit of an MDR-13 monochromator. To provide operation of the photodiodes and spectrometer in the linear regime, the radiation at their inputs was attenuated by a sequence of metal nets.

In the experiments we also recorded the voltages U_d across the laser gap, the voltages U_1 across the peaking capacitance and SOS diodes, the discharge currents I_d, the currents I_D through the diodes, and the currents in the contours of storage (I_0) and peaking (I_1) capacitances using ohmic voltage dividers, shunts, and Rogowski loops. Electric signals were applied to TDS-3034 oscilloscopes.

3. Results and discussion

3.1. Specific features of pumping a nitrogen laser by GOS

The specific features of pumping a nitrogen laser by GOS and LC generator are presented in Fig. 2. Let us consider in more detail GOS pumping (Fig. 2a; the stage of direct pumping of diodes is omitted). After operation of the SW_0 discharger a reverse current begins to flow through the diodes in the C_0–L_0–D–SW_0 circuit. The resistance of the diodes begins to grow, and approximately 25 ns later the current through the diodes drops. During this time some part of the energy accumulated in the storage capacitor, $E_L = L_0 I_{max}^2/2$ (I_{max} is the maximum reverse current through the diodes), is transferred to the inductance L_0 (inductive energy storage, IES). For the conditions shown in Fig. 2, I_{max} = 18 kA, and 10% energy stored in C_0 is transferred to IES. The current through the diodes becomes zero 40 ns after applying a reverse current to SOS. The voltage drop across the inductance L_2 changes the polarity of the voltage across the diodes after ~150 ns, inducing again current through the SOS. At the same time, the inductance L_2 begins to discharge (through the diodes) on the laser gap, as a result of which the current pulse width somewhat increases in comparison with the half-period of current oscillations in the C_0 contour.

When the diode resistance begins to increase, the IES current flows to charge the peaking capacitors. As a result the IES charges C_1 for ~15 ns to a voltage $U_0 > 40$ kV, thus providing a large E_0/p value for the laser gap. After the laser breakdown the current I_0, which remains in the inductance L_0, is summed with the current I_1 of the peaking capacitors to provide a fast increase in the discharge current and form a high-power short pump peak. The lasing pulse consists of two peaks with a dip between them, which is due to the repeated increase in the voltage across the gap.

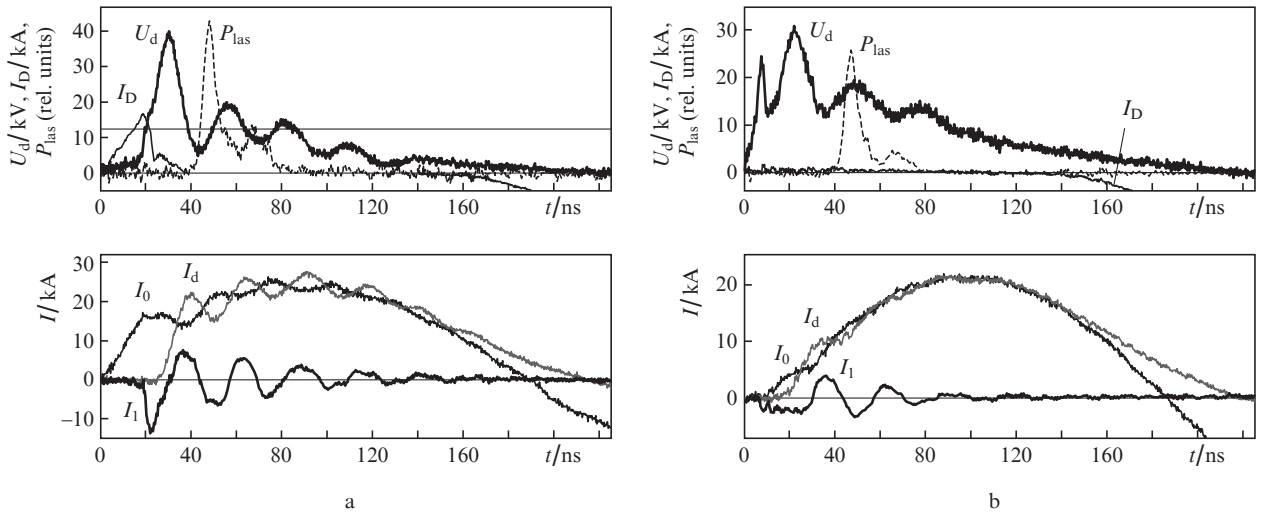

Figure 2. Oscillograms of voltage pulses U_d across the laser gap, lasing power P_{las} at λ = 337.1 nm, current I_D through SOS diodes, discharge current I_d, and currents in the circuit of storage (I_0) and peaking (I_1) capacitors under pumping a N_2 : SF_6 = 25 : 1 mixture at a pressure of 30 Torr by (a) GOS and (b) LC generator; $\mathcal{L}$ = 72 cm, U_0 = 33 kV. The horizontal line corresponds to E/p = 100 V cm^{-1} Torr^{-1}.

In the case of pumping by an LC generator (Fig. 2b) the peaking capacitors C_1 are charged only by the capacitor C_0, as a result of which the rise time of the voltage across the laser gap increases to ~40 ns, while the breakdown voltage decreases to 30 kV. The rate of discharge current rise and the amplitude of the first pump peak are reduced significantly. This leads to a twofold decrease in the energy introduced into the active medium during laser-gap voltage decay at $E/p > 100$ V cm^{-1} Torr^{-1}, in comparison with GOS pump. As a result the use of GOS to pump even pure nitrogen increases the lasing energy on the $C^3\Pi_u - B^3\Pi_g$ band by a factor of about two.

The lasing energy changes more significantly (depending on the generator type) when mixtures of nitrogen with SF_6 and NF_3 are pumped. The use of an LC generator under the conditions presented in Fig. 2 reduced the lasing energy by an order of magnitude. This is related to the discharge contraction, which is confirmed by the detection of spark channels in the gap even during the laser pulse, as in [13–16], and the fact that the lasing power in the second peak significantly differs for the two types of generators used (at similar values of pump power). The results obtained show that an increase in the discharge voltage amplitude by a simultaneous increase in its rise rate and the rise rate of discharge current using GOS, as in [10, 21–23], greatly facilitates the formation of a volume discharge and increases the duration of the volume discharge stage in mixtures of nitrogen with electronegative gases.

3.2. Energy and spectral characteristics of nitrogen laser

Figure 3 shows the dependences of the nitrogen laser energy on the charge voltage of the C_0 storage and the SF_6 concentration. The maximum lasing energy was obtained in a mixture of nitrogen and SF_6 with partial pressures of 30 and 9 Torr, respectively. The optimal SF_6 content (partial pressure) for lasing on the first positive system of nitrogen turned out to be 3 Torr. For a cavity based on an aluminum mirror and KRS-6 crystal, IR radiation energy up to 27 mJ at a peak power of 0.7 MW was obtained. The highest UV lasing energy (with a selective cavity composed of a dielectric mirror with a reflectance above 99% at 337.1 nm and a quartz plate) reached 50 mJ at a peak lasing power of 1 MW. The parameters obtained are maximum for a nitrogen laser with UV preionisation and transverse-discharge pumping. The lasing efficiency with respect to the voltage applied exceeded 0.05%. Note that only 50% energy stored in C_0 was introduced into the active medium by the end of UV lasing; therefore, the laser efficiency can be increased by shortening the pump pulse.

In the UV lasing spectrum for the optimal mixture most energy is emitted at $\lambda = 337.1$ nm (the 0–0 vibrational transition of the $C^3\Pi_u - B^3\Pi_g$ band). Weak bands (1–0), (0–1), (0–2), and (1–2) are also observed, whose contribution to the lasing energy is about 1%. Similar spectra were observed for pure nitrogen and mixtures with NF_3, which suggests similarity of the processes of attaining inversion on the $C^3\Pi_u - B^3\Pi_g$ transition under given conditions [10].

The nitrogen laser emission on the first positive system in the optimal gas mixture included the (2–1), (1–0), and (0–0) transitions with wavelengths of 869.5, 888.3, and 1046.9 nm and close intensities. Addition of helium in small amounts led to an increase in the intensity of the (0–0) transition and disappearance of the two other transitions. This can be related to the collisional quenching of levels with the vibrational numbers $v = 2$ and 1. With an increase in the SF_6 concentration we observed a rise in the intensity of the (2–1) transition and a decrease in the (0–0)-transition intensity, whereas the total IR lasing energy decreased.

The experiments revealed a strong dependence of the IR laser energy on the volume discharge homogeneity. The formation of spark channels led to a sharp decrease in the IR intensity because of low gain at the IR transitions and inhomogeneities in the active medium of the laser. Lasing at the IR transitions began about 30 ns after the beginning of the UV pulse. By that instant, at a high concentration of electronegative additive, the discharge lost homogeneity even when using GOS. The effect of discharge homogeneity on the radiation energy for the first positive system was most pronounced in mixtures with NF_3 (Fig. 4). At an NF_3 partial pressure of 0.5 Torr, GOS forms a uniform discharge more than 150 ns long. In this case, the lasing energies were the same for the first and second positive nitrogen systems. With an increase in the NF_3 concentration the discharge loses homogeneity and

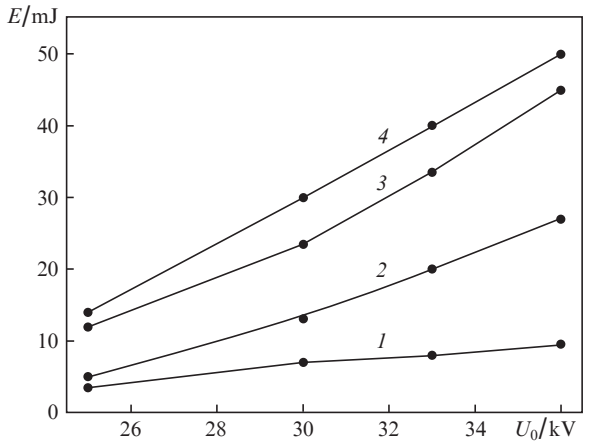

Figure 3. Dependences of the nitrogen laser energy for the (*1*,*3*,*4*) second and (*2*) first positive nitrogen systems on the charge voltage across the capacitance C_0 for (*1*) nitrogen at $p = 60$ Torr and mixtures $N_2:SF_6$ = (*2*) 30:3, (*3*) 60:7.5, and (*4*) 30:9 (in Torr); $\mathcal{L} = 90$ cm, the cavity is formed by (*1*,*3*,*4*) a mirror with a reflectance above 99% at 337.1 nm and a quartz plate and (*2*) an Al mirror and a KRS-6 crystal.

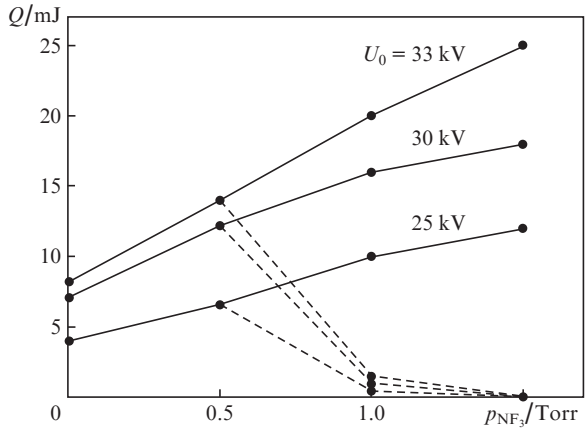

Figure 4. Dependences of the nitrogen laser energy for the (solid lines) second and (dashed lines) first positive nitrogen systems on the NF_3 pressure at a nitrogen pressure of 60 Torr. The nonselective cavity is formed by an Al mirror and a quartz plate; $\mathcal{L} = 90$ cm.

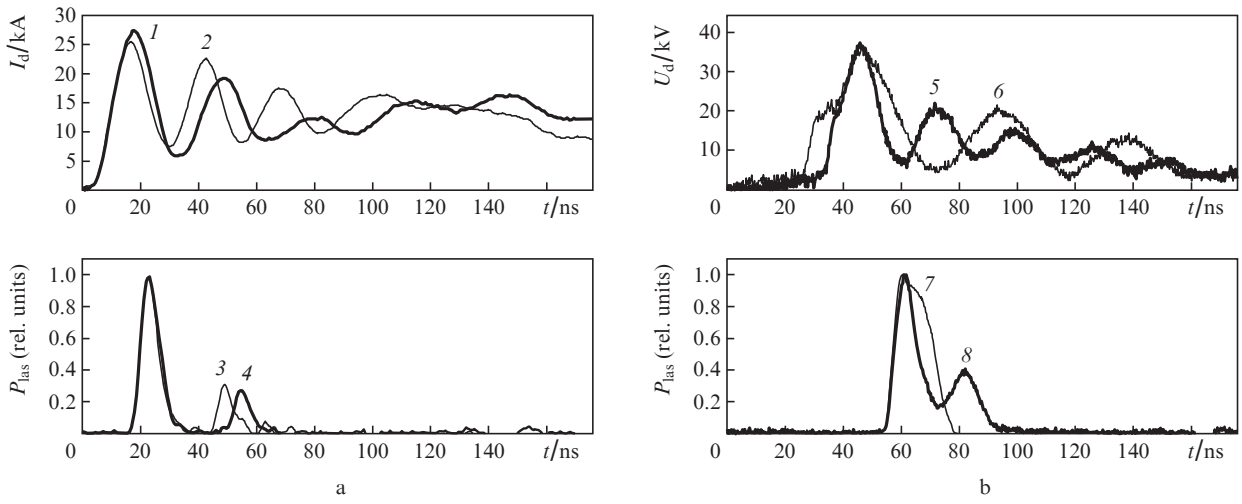

Figure 5. Oscillograms of (*1*, *2*) discharge current pulses, (*5*, *6*) the voltage across the laser gap, and (*3*, *4*, *7*, *8*) the laser power at λ = 337.1 nm in mixtures (a) N_2 : NF_3 = 75 : 3 and (b) N_2 : SF_6 = 30 : 3 (in Torr) at C_1 = (*2*, *3*, *5*, *8*) 2.45, (*1*, *4*) 3.6, and (*6*, *7*) 7.2 nF; $\mathcal{L}$ = 72 cm, U_0 = 33 kV.

begins to expand from the centre of the laser gap to its edges (this phenomenon will be discussed in more detail below). As a result the IR lasing energy decreases to zero, whereas the UV energy continues to grow. Similar dependences were obtained for SF_6-containing mixtures with an increase in the additive pressure from 3 to 9 Torr. Under LC-generator pumping the lasing energy at the first positive nitrogen system did not exceed 1 mJ because of the fast discharge contraction.

3.3. Two-spike regime of nitrogen laser

A characteristic feature of lasing on nitrogen mixtures with SF_6 and NF_3 additives is the generation of a two-peak pulse (Fig. 2). This is related to the increase in the discharge burning voltage due to the attachment of electrons to additive molecules and modulation of the voltage across the laser gap by oscillations of the peaking-capacitance current. The amplitude U_d of the second peak corresponds to $E/p > 100$ V cm^{-1} Torr^{-1}, which is sufficient for periodic formation of inverse population on the $C^3\Pi_u - B^3\Pi_g$ transition in the active medium of nitrogen laser. The depth of the dip between the lasing peaks depends on the mixture pressure. With an increase in pressure, for ~10% additive and $\mathcal{L}$ = 72 cm, a two-peak lasing pulse was observed, as in [6, 10]. Similar voltage oscillations are observed for pure nitrogen; however, without an electronegative impurity, the E/p value for the second voltage peak (below 40 V cm^{-1} Torr^{-1}) is too small to obtain inverse population in the $C^3\Pi_u - B^3\Pi_g$ system. At the same time, one can control the laser pulse shape by changing the oscillation period of the peaking-contour current. The effect of C_1 on the pulse shape is shown in Fig. 5. With an increase in the peaking capacitance from 2.45 to 3.6 nF the modulation period of the discharge current increased from 25 to 33 ns. Accordingly, the distance between the lasing peaks increased. A further increase in the oscillation period to 45 ns led to the disappearance of the second lasing peak, which is related to a complete loss of inversion of the populations of $C^3\Pi_u - B^3\Pi_g$ transition during this time interval [10].

The delay between the lasing peaks increased even more in NF_3-containing mixtures due to the increase in the current oscillation period in the C_1 circuit and redistribution of the discharge current density. With increasing the NF_3 concentration, decreasing the charge voltage of the capacitor C_0, and (or) switching off SOS, the first lasing peak arises at the centre of the discharge gap, whereas the second peak shifts to the boundaries of the discharge region. Since the threshold discharge current density in nitrogen laser is ~100 A cm^{-2} [13–16], this phenomenon can be related to the displacement of the discharge region with a maximum current density from the laser gap centre to the periphery during pumping (Fig. 6). The discharge current redistribution over the laser gap width makes it possible to increase the delay between the peaks and the total pulse width of nitrogen laser to ~60 ns.

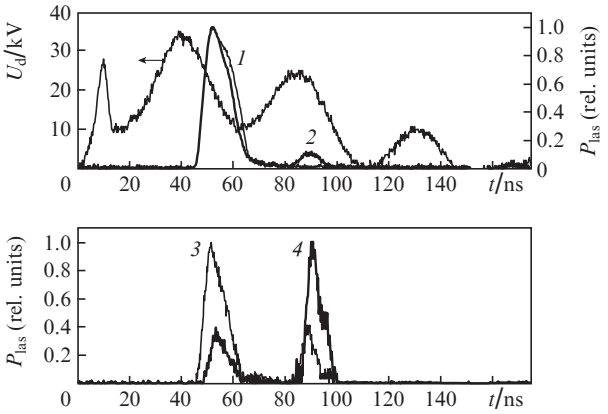

Figure 6. Oscillograms of voltage pulses across the laser gap and the laser power at λ = 337.1 nm in a N_2 : NF_3 = 25 : 1 mixture at p = 45 Torr. Radiation was recorded from (*1*) the discharge gap centre, (*2*) the entire laser aperture, and (*3*, *4*) the regions spaced by (*3*) 5 and (*4*) 8 mm from the centre of the laser gap. Pumping by an LC generator, C_1 = 7.2 nF, U_0 = 33 kV, $\mathcal{L}$ = 72 cm.

The generation of lasing peaks from different discharge regions, which is related to discharge expansion, can be explained by the nonmonotonic dependence of the attachment coefficient of NF_3 molecules on the electron energy [24] and the E/p ratio [10]. Note that lasing in different discharge regions was observed only under the conditions where the pump generator could not provide a fast increase in the discharge current

[high NF_3 concentration, absence of SOS, and (or) low U_0]. Because of the electrode geometry the E/p value is somewhat larger at the centre of the discharge gap. In this case, during voltage decay the current density will be maximum near the laser gap centre. At the instant of gap breakdown E/p exceeds 80 V cm^{-1} Torr^{-1}, a value at which the electron attachment rate constant and the attachment cross section of NF_3 molecules are maximum [10]. In this context, the electron attachment rate of NF_3 monotonically decreases with an increase in E/p and becomes minimum in the central part of the laser gap, which leads to a maximum discharge current density in this region. At a repeated increase in voltage the electron attachment coefficient in the central region of the discharge increases more rapidly than at the periphery; therefore, the discharge current density begins to increase at the edges of the discharge aperture, which leads to the formation of the second lasing peak at the edges of the discharge region. The similar behavior of the discharge in a wide-aperture nitrogen laser increases the laser pulse width to ~100 ns [25].

The attachment coefficient in N_2–SF_6 mixtures monotonically decreases with an increase in E/p [26]; therefore, in SF_6-containing mixtures and (under optimal pumping conditions) in mixtures with NF_3 a discharge is formed over the entire gap width during few nanoseconds, and lasing begins simultaneously over the entire discharge aperture. No significant redistribution of the current density is observed in this case.

3.4. Generation of rectangular pulses on the $C^3\Pi_u$–$B^3\Pi_g$ transition

Figure 7 shows the oscillograms of the voltage pulses across the laser gap and lasing pulses at λ = 337.1 nm, which were obtained for nitrogen–SF_6 mixtures at $\mathcal{L}$ = 90 cm. Since the oscillation period of the laser gap voltage was the same for the two lasers, the disappearance of the dip between the peaks, which were observed under the experimental conditions indicated in Figs 2 and 5, is related to the increase in $\mathcal{L}$. The shape of the lasing pulses was close to rectangular, and their full width reached 55 ns. The full width at half maximum of about 35 ns was obtained at an additive pressure of 4.5 Torr and the lasing energy close to maximum (Fig. 3).

Lasing pulses with a width of about 50 ns were also produced at $\mathcal{L}$ = 72 cm at a low mixture pressure [6, 10]; however, the lasing energy was below 10 mJ in this case. The amplitude of the second voltage peak across the laser gap in the range of additive pressures of 4.5–9 Torr changed only slightly; therefore, some decrease in the lasing pulse width at half maximum with an increase in the SF_6 concentration is related to the decrease in the E/p parameter in the second peak of U_d. The lasing energy on IR transitions in nitrogen did not exceed 2–3 mJ in these experiments.

3.5. Cascade lasing in the nitrogen laser

The cascade lasing in the nitrogen laser was investigated in [27–29]. However, in these studies only the effect of laser radiation at the $C^3\Pi_u$–$B^3\Pi_g$ band on only the population of the upper laser level of the $B^3\Pi_g$–$A^3\Sigma_u^+$ band was considered, because UV lasing always ceased a long time before the threshold for IR transitions was obtained.

In our experiments with $\mathcal{L}$ = 90 cm and a nonselective cavity composed of an aluminum mirror and quartz plate, an interesting result was obtained in mixtures of nitrogen with small amounts of NF_3 and SF_6, which suggests the effect of IR lasing on the lasing parameters at λ = 337.1 nm. With an increase in $\mathcal{L}$ the lasing on the first and second positive nitrogen systems was observed simultaneously (Fig. 8). First, as in all previous experiments, the lasing threshold was obtained at λ = 337.1 nm, and then an IR pulse arose (before the lasing power on the second positive nitrogen system decreased significantly). The full width of the UV pulse reached 100 ns, and the energy in its tail was about 3% of the total energy. Simultaneous lasing on two positive nitrogen systems was previously observed in [30]; however, when a strip-line generator was used, the widths of the pump and UV pulses did not exceed ~10 ns. The main condition for the increase in the lasing pulse width at λ = 337.1 nm was the high lasing energy on the first positive nitrogen system (comparable with the UV lasing energy). For the conditions indicated in Figs 4 and 8 the lasing energies in the UV and IR bands were 12–14 mJ. When using a selective cavity with a mirror having a reflectance of above 99% at λ = 337.1 nm or at a small misalignment of nonselective cavity (in order to reduce the feedback coefficient), lasing on IR transitions began after the end of the UV pulse, and its energy decreased by an order of magnitude. The IR lasing energy decreased also as a result of violation of discharge homogeneity when using an LC generator and (or) mixtures

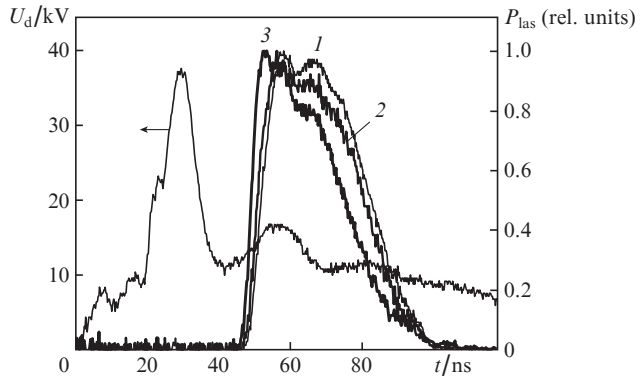

Figure 7. Oscillograms of a voltage pulse across the laser gap and the laser power at λ = 337.1 nm in a mixture of nitrogen (p = 30 Torr) with SF_6 additives at pressures of (*1*) 4.5, (*2*) 6, and (*3*) 9 Torr; U_0 = 33 kV, $\mathcal{L}$ = 90 cm.

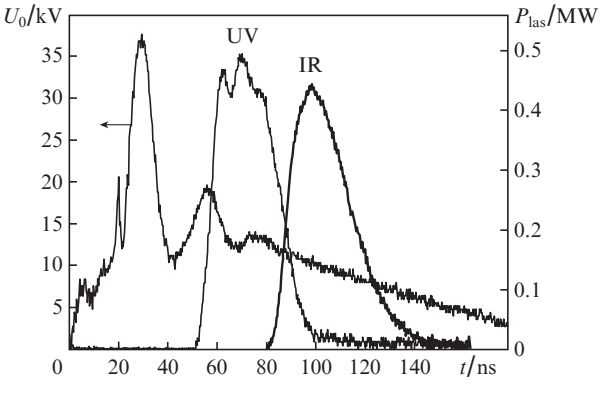

Figure 8. Oscillograms of a voltage pulse across the laser gap and the laser power for the first (IR) and second (UV) positive nitrogen systems in a N_2:SF_6 = 30:3 (in Torr) mixture at U_0 = 33 kV and $\mathcal{L}$ = 90 cm (nonselective cavity).

with a high content of electronegative additives. Under these conditions, the lasing pulse width at λ = 337.1 nm did not increase (Fig. 7). Note that this result is not related to the detection of spontaneous radiation, because the measurements were performed at a distance of 3–5 m from the laser. When no optical cavity was used and only accelerated spontaneous radiation was produced, the photocells recorded no signals.

The increase in the UV lasing pulse width can be explained by the depletion of the lower laser $B^3\Pi_g$ level of the second positive system via induced cascade transitions in the $B^3\Pi_g - A^3\Sigma_u^+$ band of the first positive system. At similar lasing energies the $B^3\Pi_g$ level will be depleted three times faster due to the transitions in the first positive system than populated as a result of UV lasing. Apparently, this is not sufficient for preserving the population inversion on the $C^3\Pi_u - B^3\Pi_g$ transition, and an increase in $\mathcal{L}$ makes it possible to increase the UV lasing pulse width to 100 ns.

4. Conclusions

We investigated the lasing parameters in mixtures of nitrogen with electronegative impurities under pumping by a transverse discharge from different generators. It was shown that a stable volume discharge is formed in N_2–SF_6 (NF_3) mixtures when GOS is used; this circumstance allows one to increase the lasing energy and efficiency on the first and second positive nitrogen systems and implement different working regimes of UV nitrogen laser. The lasing energy in the wavelength range of 869.5–1047 nm reached 27 mJ at a peak power of 0.7 MW, and the lasing energy at λ = 337.1 nm was 50 mJ (with a peak power of 1 MW).

The width of induced lasing pulse at λ = 337.1 nm was significantly increased. The highest lasing energies on the first and second positive nitrogen systems were obtained under pumping by a transverse discharge with UV preionisation.

The regime of two-peak laser pulses with a controlled delay between the peaks was implemented. It was shown that the delay between the peaks may exceed 50 ns for a mixture of nitrogen with NF_3.

The conditions for attaining effective UV lasing with a total pulse width of more than 50 ns were determined. Simultaneous lasing on the first and second positive nitrogen systems was obtained. It was shown that the lower level of the $C^3\Pi_u - B^3\Pi_g$ transition can be depleted by induced transitions of the second positive $B^3\Pi_g - A^3\Sigma_u^+$ system, due to which the pulse width can be increased to 100 ns at λ = 337.1 nm.

Acknowledgements. This study was supported in part by the Federal Target Program 'Scientific and Scientific-Pedagogical Personnel of Innovative Russia' (State Contract No. 02.740.11.0562).

References

1. Gushchin E.M., Mikhanchuk N.A., Pokachalov S.G. *Pis'ma Zh. Tekh. Fiz*., **31**, 42 (2005).
2. Zhu C., Palmer G.M., Breslin T.M., Harter J., Ramanujam N. *J. Biomed. Opt.*, **13**, 034015 (2008).
3. Gheysari Z., Jelvani S., Abolhosseini Sh., Rouhollahi A., Vatani V., Rabbani M. *Int. J. Electrochem. Sci.*, **5**, 242 (2010).
4. Bulgakova N.M., Panchenko A.N., Tel'minov A.E., Shulepov M.A. *Appl. Phys. A: Mater. Sci. Proc.*, **98**, 393 (2010).
5. Bahrampour Alireza, Fallah R., Ganjovi A.A., Bahrampour Abolfazl. *Opt. Las. Technol.*, **39**, 1014 (2007).
6. Panchenko A.N., Suslov A.I., Tarasenko V.F., Tel'minov A.E. *Kvantovaya Elektron.*, **37**, 433 (2007) [*Quantum Electron*., **37**, 433 (2007)].
7. Hariri A., Jaberi M., Ghoreyshi S. *Opt. Commun.*, **281**, 3841 (2008).
8. Kozyrev A.V., Panchenko A.N., Tarasenko V.F., Tel'minov A.E. *Kvantovaya Elektron*., **38**, 731 (2008) [*Quantum Electron*., **38**, 731 (2008)].
9. Razhev A.M., Churkin D.S, and Zhupikov A.A. *Kvantovaya Elektron.*, **39**, 901 (2009) [*Quantum Electron*., **39**, 901 (2009)].
10. Panchenko A.N., Suslov A.I., Tarasenko V.F., Konovalov I.N., Tel'minov A.E. *Phys. Wave Phenomena*, **17**, 251 (2009).
11. Tarasenko V.F. *Kvantovaya Elektron*., **31**, 489 (2001) [*Quantum Electron*., **31**, 489 (2001)].
12. Bychkov Yu.I., Losev V.F., Savin V.V., Tarasenko V.F. *Izv. Vyssh. Uchebn. Zaved., Ser. Fiz.*, (1), 81 (1978).
13. Levatter J.I., Lin S.-C. *Appl. Phys. Lett.*, **25**, 703 (1974).
14. Rebhan U., Hildebrandt J., Skopp G. *Appl. Phys. A: Mater. Sci. Proc.*, **23**, 341 (1980).
15. Buranov S.H., Gopokhov B.B., Kapelin B.I., Pepin P.B. *Kvantovaya Elektron*., **17**, 161 (1990) [*Sov.J. Quantum Electron*., **20**, 120 (1990)].
16. Armandillo E., Kearsley A.J. *Appl. Phys. Lett*., **41**, 611 (1982).
17. Sanz F.E., Guerra Perez J.M. *Appl. Phys. B*, **52**, 42 (1991).
18. Judd O.P. *IEEE J. Quantum Electron*., **12**, 78 (1976).
19. Suchard S.N., Sutton D.G., Heidner R., III. *IEEE J. Quantum Electron.*, **11**, 908 (1975).
20. Suchard S.N., Galvan L., Sutton D.G. *Appl. Phys. Lett*., **26**, 521 (1975).
21. Bychkov Yu.I., Panchenko A.N., Tarasenko V.F., Tel'minov A.E., Yampol'skaya S.A., Yastremskii A.G. *Kvantovaya Elektron*., **37**, 319 (2007) [*Quantum Electron*., **37**, 319 (2007)].
22. Bychkov Yu.I., Panchenko A.N., Tarasenko V.F., Tel'minov A.E., Yampol'skaya S.A., Yastremskii A.G. *Izv. TPU*, **312**, 113 (2008).
23. Orlovskii V.M., Panchenko A.N., Tarasenko V.F. *Kvantovaya Elektron.*, **40**, 192 (2010) [*Quantum Electron*., **40**, 192 (2010)].
24. Nandi D., Rangwala S.A., Kumar S.V.K., Krishnakumar E. *Int. J. Mass Spectrometry*, **205**, 111 (2001).
25. Konovalov I.N., Panchenko A.N., Tarasenko V.F., Tel'minov E.A. *Kvantovaya Elektron*., **37**, 623 (2007) [*Quantum Electron*., **37**, 623 (2007)].
26. Christophorou L.G., Oltoff J.K. *J. Phys. Chem. Ref. Data*, **29**, 267 (2000).
27. Lisitsyn B.H., Copokin A.P., Telegin G.G. *Kvantovaya Elektron.*, **2**, 1710 (1975) [*Sov. J. Quantum Electron*., **5**, 927 (1975)].
28. Yasuda Y., Sokabe N., Murai A. *Jpn. J. Appl. Phys*., **19**, 1143 (1980).
29. Scaffardi L., Schinca D., Tocho J.O., Ranea-Sandoval H.F., Gallardo M. *Appl. Opt.*, **11**, 22 (1985).
30. Tarasenko B.F., Bychkov Yu.I. *Zh. Tekh. Fiz*., **44**, 1100 (1974).